JOURNAL OF MACROMOLECULAR SCIENCE, PART A: PURE AND APPLIED CHEMISTRY
https://doi.org/10.1080/10601325.2021.1934012

Photodynamic therapy activities of phthalocyanine-based macromolecular photosensitizers on MCF-7 breast cancer cells

Erem Ahmetali[a], Pinar Sen[b], N. Ceren Süer[a], Tebello Nyokong[b], Tarik Eren[a], and M. Kasım Şener[a]

[a]Department of Chemistry, Yıldız Technical University, İstanbul, Turkey; [b]Department of Chemistry, Rhodes University, Grahamstown, South Africa

ABSTRACT

Poly(oxanorbornene)s with zinc(II) phthalocyanine side chains have been synthesized by ring-opening metathesis polymerization. The incorporation of zinc(II) phthalocyanine into cationic polymer has given poly(oxanorbornene)s noteworthy photophysicochemical properties and the capacity to generate singlet oxygen under light irradiation. To investigate photosensitizer's properties of the newly synthesized polymers **P6** and **P7**: fluorescence (Φ_F), singlet oxygen (Φ_Δ) and triplet (Φ_T) quantum yields of polymers have been measured in dimethyl sulfoxide and aqueous medium. Singlet oxygen quantum yields of **P6** and **P7** have been found to be 0.22 and 0.20 in dimethyl sulfoxide, respectively. Then, photodynamic therapy activities of polymers (**P1-P7**) against human breast adenocarcinoma cell line (MCF-7 cells) have been investigated. The copolymer **P5** bearing pendant zinc(II) phthalocyanine and triethyl phosphonium functionalities has showed enhanced PDT activity with less than 10% viable cells at 60 μg/mL.

GRAPHICAL ABSTRACT

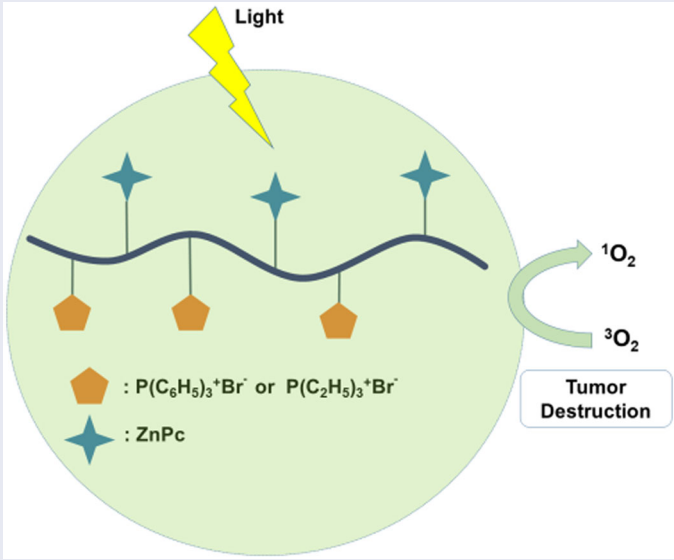

ARTICLE HISTORY
Received March 2021
Accepted May 2021

KEYWORDS
Macromolecular photosensitizer; phthalocyanine; photodynamic therapy; poly(oxanorbornene); triphenylphosphonium

1. Introduction

From past to present, cancer is one of the foremost diseases to be treated. There are two major medicinal methods in the cancer treatment and these methods can be classified as chemotherapy and radiotherapy. However, since cancer cells and normal cells can be synchronously affected as a negative by the abovementioned treatments, researchers have continued to study on more harmless and efficient treatments.[1,2]

Nowadays, a promising approach for the cancer therapy has emerged which make use of photoirradiation to uproot hostile cells called as photodynamic therapy (PDT). As compared to conventional chemotherapy and radiotherapy, photodynamic therapy (PDT) has the advantages of non-invasiveness, minimal side effects, and relatively high therapeutic selectivity.[3–5] PDT consist of two steps. In the first step, the photosensitizer (PS) is given to the patient's body.

CONTACT M. Kasım Şener mkasimsener@gmail.com Department of Chemistry, Yıldız Technical University, 34210 İstanbul, Turkey; Tarik Eren erentari@gmail.com Department of Chemistry, Yıldız Technical University, 34210 İstanbul, Turkey; Tebello Nyokong t.nyokong@ru.ac.za Department of Chemistry, Rhodes University, 6140 Grahamstown, South Africa.

Secondly, a light beam, which has convenient wavelength, is applied to the tissue. The PS absorbs a photon and gives rise to fluorescence emission. As a result, molecular oxygen in the tissues turns into singlet molecular oxygen ($^1O_2$). This is responsible for eradicating the target cells.

PSs are synthetic or natural chemicals that participate as light absorbing species in PDT processes.[6] Borondipyrromethene (BODIPY),[7,8] porphyrin (Por),[9,10] and phthalocyanine (Pc)[11–14] possess pyrrole subunits, and are the most studied compounds as PS in the literature. Pcs have stood out with their long absorption wavelength maxima, high extinction coefficients and high singlet oxygen generation among these molecules. Although they are suitable candidates as PS for PDT, they have some negative characteristics such as planarity and hydrophobicity that lead to the formation of aggregates in aqueous medium.[15] This situation dramatically reduces the photodynamic activity of PS against tumor.[16] These could be overcome by incorporating into polymers with hydrophilic character to enhance the PSs solubility in physiological medium.[15,17,18] Also, small sized nanoparticles and macromolecular PSs can accumulate more in solid tumors than in normal tissues which is known as the enhanced permeability and retention (EPR) effect. The PSs can be incorporated into polymers to increase the blood circulation time and prevent renal clearance for more efficient accumulation in the solid tumor via the EPR effect.[19,20] The anti-cancer activity can be enormously enhanced by polymerization of the PSs that take part as drugs in PDT, and thus, they act as "macromolecular photosensitizers" (MPSs).[21–25]

The physicochemical properties of the PSs, such as chemical structure, and charge also play a critical role on their accumulation in cell structures or organelles such as lysosome and mitochondria. The mitochondria is an attractive and important target for PDT because of its central role in energy metabolism and regulation of apoptosis. PSs which contain cationic groups can able to target mitochondria since the mitochondrial matrix has a highly negatively charged microenvironment and thus apoptosis can be ensured to happen.[26–29] Related studies have been carried out by introducing rhodamine[30,31] and triphenyl phosphine groups[32] as cationic actor to phthalocyanine ring. The most well-known mitochondria-targeting units is the triphenylphosphonium moiety which is used in MitoTrackers such as MitoSOX^{TM} Red reagent. Moreover, there is only one study that been reported as mitochondrion-targeting phthalocyanine with triphenylphosphonium groups in the literature.[32] Recently, we have synthesized phthalocyanine-based macromolecular photosensitizers containing mitochondria-targeting phosphonium groups and examined their photodynamic antimicrobial chemotherapy (PACT) activities.[33] The polymers we have obtained were the first example of macromolecular photosensitizers in the literature. Herein, two additional polymers were synthesized to complete polymer series and their photodynamic therapy activities on MCF-7 breast cancer cells are compared as a continuation of our work (Figure 1).

2. Experimental section

2.1. Chemicals and reagents

All reagents and solvents were of reagent grade quality and were obtained from commercial suppliers. 1,3-diphenylisobenzofuran (DPBF) and 9,10-anthracenediyl-bis(methylene)-dimalonic acid (ADMA) were obtained from Sigma-Aldrich. Phosphate-buffered saline (PBS) solution (pH 7.4) was prepared using appropriate amounts of Na_2HPO_4 and KH_2PO_4 in ultra-pure water from a Millipore water was from ELGA, Veolia water PURELAB, flex system (Marlow, UK).

MCF-7 breast cancer cells were obtained from Cellonex. Dulbecco's phosphate-buffered saline (DPBS) and Dulbecco's modified Eagle's medium (DMEM) with phenol red, phenol red free DMEM, Dulbecco's phosphate–buffered saline (DPBS) and trypsin were purchased from Sigma-Aldrich. 100 μg/mL–penicillin–100 unit/mL–streptomycin–amphotericin B mixture, heat-inactivated fetal bovine serum (FBS) were acquired from Biowest®. Cell proliferation neutral red reagent WST–1 (Roche®), 96 well cell culture plates (Nest®), and 75 cm^2 vented flasks were obtained from Porvair®. The illumination kit for *in vitro* PDT studies has capacity to hold 127.76 × 85.48 mm 96 well tissue culture plate. **1** and **2** were synthesized according to the published procedures.[33,34]

2.2. Instrumentation

FT-IR spectra were recorded on a Thermo Scientific iS10 FT-IR (ATR sampling accessory) spectrophotometer and electronic spectra on a Shimadzu UV-2450. NMR spectra were recorded Agilent VNMRS 500 MHz spectrometer using TMS as an internal reference. Fluorescence emission spectra were recorded on a Varian Eclipse spectrofluorometer with quartz cell of 1 cm at room temperature. Fluorescence lifetimes were measured using a time correlated single photon counting setup (TCSPC) (FluoTime 300, Picoquant GmbH). The excitation source was a diode laser (LDH-P-670 driven by PDL 800-B, 670 nm, 20 MHz repetition rate, 44 ps pulse width, Picoquant GmbH). Triplet quantum yield values were obtained using a laser flash photolysis system having a LP980 spectrometer with a PMT-LP detector and an ICCD camera (Andor DH320T-25F03). The signal from a PMT detector was recorded on a Tektronix TDS3012C digital storage oscilloscope. The excitation pulses were produced by a tunable laser system consisting of a Nd:YAG laser (355 nm, 135 mJ/4–6 ns), pumping an optical parametric oscillator (OPO, 30 mJ/3–5 ns) with a 420 to 2300 nm (NT-342B, Ekspla) wavelength range. Photo-irradiations for singlet oxygen studies were done using a General Electric Quartz line lamp (300 W). The illumination source for the PDT studies was obtained from Modulight® Medical Laser System (MLS) 7710-680 channel Turnkey laser system coupled with a 2 × 3 W channel at 680 nm, cylindrical out-put channels, aiming beam, integrated calibration module, foot/hand switch pedal, fiber sensors (subminiature version A) connectors, and safety interlocks. The WST-1 assay was used to assess the toxicity and cell proliferation as per manufacturer's instructions

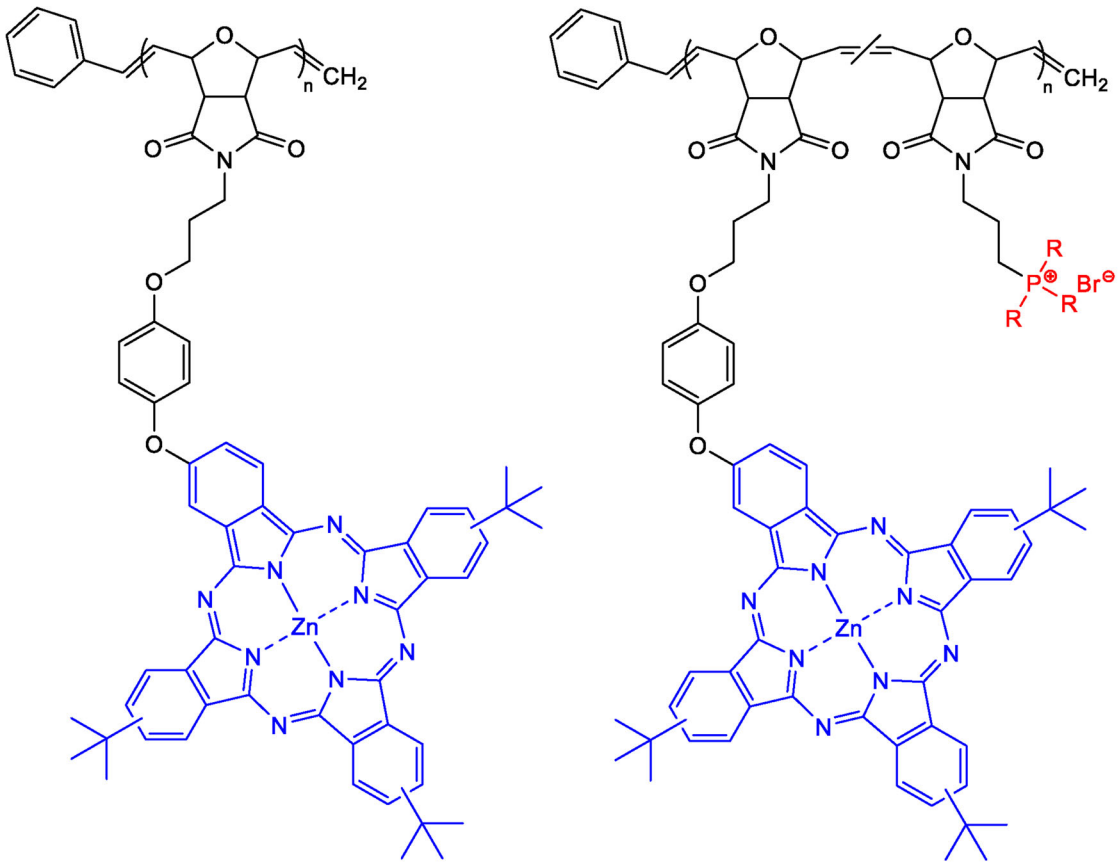

Figure 1. Structure of macromolecular photosensitizers (TPP^+: triphenylphosphonium, TEP^+: triethylphosphonium).

(Roche) using a Synergy 2 multi-mode microplate reader (BioTek®) at a wavelength of 450 nm.

2.3. In vitro dark cytotoxicity and PDT activity

The cytotoxic activity of the drugs (**P1**-**P7**) were tested against MCF-7 cells in the dark and under light as reported in the literatures.[35] Briefly, MCF-7 (human breast adenocarcinoma) cells were cultured in Dulbecco's modified Eagle's medium-10% fetal bovine serum (DMEM-FBS) and PSA (penicillin/streptomycin/Amphotericin B) at 37 °C in an incubator (5% CO_2) in 75 cm^2 vented flasks. The cultures were grown as a monolayer. The growth cells were transferred to well plates by trypsinizing with 0.25% trypsin-EDTA. The polymer stock concentrations were prepared by separately dissolving them in DMSO (1%) and diluting in water and the polymer gradient concentration was prepared by taking known aliquots from the stock and finally made up to marked volume with supplemented media with phenol red.

It was studied from 5 to 100 µM both in the dark and light. 100 µL each of the newly prepared gradient polymers (**P1**-**P7**) concentration of 0 µg/mL (control), 5 µg/mL, 10 µg/mL, 20 µg/mL, 40 µg/mL, 60 µg/mL, 80 µg/mL and 100 µg/mL were administered on the incubated seeded cells. The 96 well cell culture plates containing the cells and the polymers were incubated at 37 °C and 5% CO_2 in the dark for 24 h. After 24 h treatment, the wells were rinsed with 100 µL DPBS. Cell survival was expressed as percentage of control cells (cells without polymers). Post treatment cell viability was measured using the cell proliferation neutral red reagent (WST-1 assay) on a Synergy 2 multi-mode microplate reader (BioTek®) at a wavelength of 450 nm according to the following equation 1. Also the analyses method was given in the related studies.[36]

$$\%\mathrm{CellViability} = \frac{\mathrm{Absorbanceofsamplesat450nm}}{\mathrm{Absorbanceofcontrolat450nm}} \times 100\% \quad (1)$$

2.4. General procedure for preparation of copolymers P6 and P7

1 and **2** were dissolved in 2 mL of DMF under nitrogen atmosphere and then Grubbs' catalyst (2nd gen) in 0.5 mL of

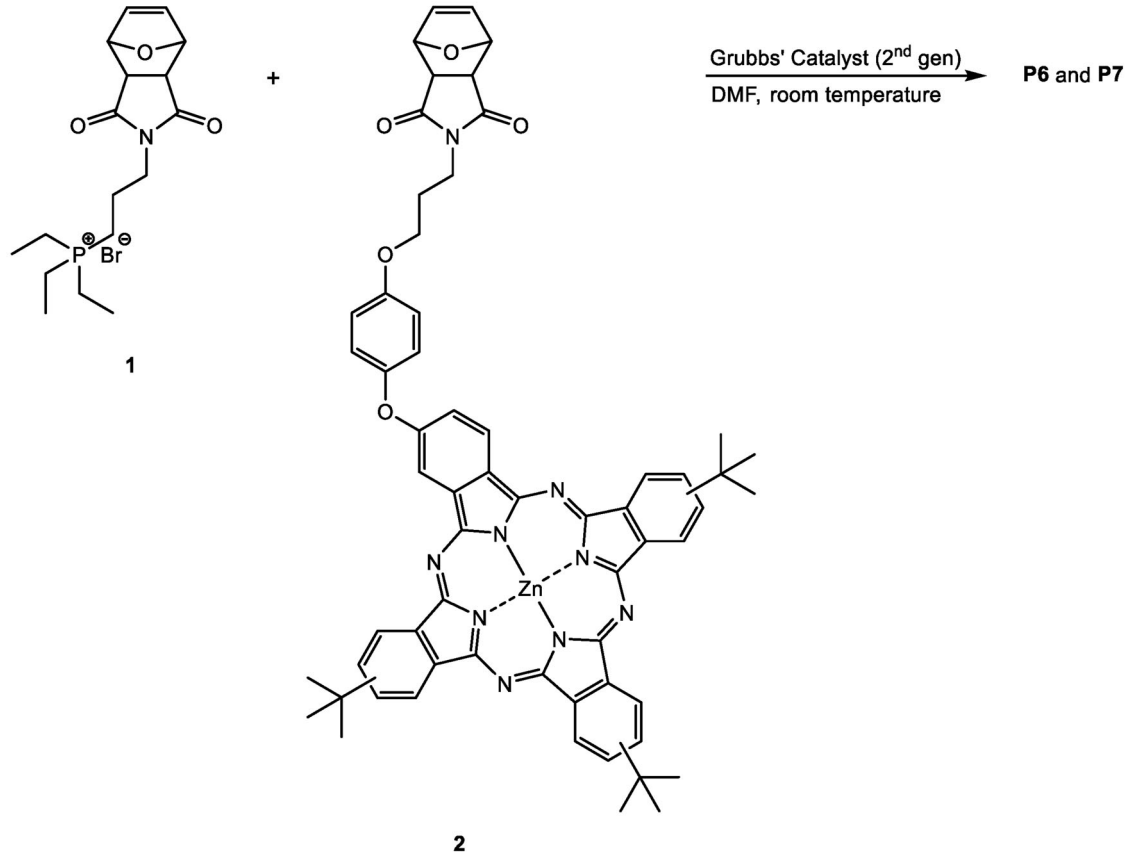

Scheme 1. Synthesis of **P6** and **P7**.

dichloromethane (DCM) was added in one shot to the stirring monomers' solution. After stirring overnight, 0.5 mL of 30% ethyl vinyl ether was added for the termination of reaction. It was then precipitated and washed with diethylether. It was dried in a vacuum oven after centrifugation. A blue colored substance was obtained.

P6: 0.015 g **1** (0.0371 mmol) and 0.015 g **2** (0.014 mmol) were used. Theoretical molecular weight = 10,000 g mol^{-1}. Yield: 0.026 g (86%). FT-IR υ_{max}: 3062.90, 2950.97, 1774.99, 1698.06, 1613.86, 1489.02, 1464.28, 1397.73, 1362.20, 1329.42, 1254.81, 1215.90, 1153.57, 1086.30, 1044.09, 938.30, 919.80, 872.66, 831.93, 762.21, 750.12 cm^{-1}. UV-Vis (DMSO) λ_{max}: 678, 613, 350 nm. ^{1}H-NMR (DMSO-d_6) δ: 9.41-7.10 (Ar), 5.96 (a cis), 5.75 (b trans), 4.90 (c cis), 4.43 (c trans), 4.08 (CH_2), 3.62 (CH_2), 2.16 (CH_2CH_3), 1.75 ($C(CH_3)_3$), 1.02 (CH_3) ppm. ^{31}P-NMR (DMSO-d_6) δ: 39.23 ppm.

P7: 0.0085 g **1** (0.0210 mmol) and 0.020 g **2** (0.0187 mmol) were used. Theoretical molecular weight = 10,000 g mol^{-1}. Yield: 0.018 g (63%). FT-IR υ_{max}: 3066.77, 2953.54, 1775.63, 1698.67, 1612.04, 1488.76, 1469.27, 1394.38, 1363.02, 1329.25, 1280.40, 1255.22, 1215.91, 1152.24, 1085.77, 1044.25, 938.12, 919.80, 872.22, 830.60, 761.12, 749.51 cm^{-1}. UV-Vis (DMSO) λ_{max}: 678, 613, 348 nm. ^{1}H-NMR (DMSO-d_6) δ: 9.42-7.11 (Ar), 5.95 (a cis), 5.74 (b trans), 4.90 (c cis), 4.45 (c trans), 4.08 (CH_2), 3.45 (CH_2), 2.09 (CH_2CH_3), 1.77 ($C(CH_3)_3$), 0.96 (CH_3) ppm. ^{31}P-NMR (DMSO-d_6) δ: 39.32 ppm.

3. Results and discussion

3.1. Synthesis

Poly(oxanorbornene)s **P1**-**P5** were synthesized according to the procedure from that previously reported by our group.[33] In this study, **P6** and **P7** were obtained by ring-opening metathesis polymerization (ROMP) of the pre-prepared monomers **1** and **2** for comparison. As shown in Scheme 1, copolymerization of **1** with phthalocyanine-containing monomer **2** in N,N-dimethylformamide (DMF) in the presence of Grubbs' Catalyst (2nd gen) at room temperature afforded the **P6** and **P7** with varying composition.

The formation of copolymers was confirmed by appearance of new broad cis/trans peaks at around 5.7-5.9 ppm for the polymer backbone and the disappearance of the typical peaks belong to monomers at around 5.2 and 6.5 ppm in the ^{1}H-NMR spectra of **P6** and **P7**, which is consistent with the reported values for poly(oxanorbornene)s (Figure 2a).[34,37]

^{31}P-NMR, FT-IR and UV-Vis spectroscopic techniques provided the additional evidence for the formation of copolymers. In the ^{31}P-NMR spectra of copolymers **P6** and **P7**, one peak was observed at 39 ppm for triethylphosphonium groups (Figure 2b).

In the FT-IR spectra of **P6** and **P7**, aromatic and aliphatic C-H stretching vibrations and C = O stretching vibration were observed at ~3060, ~2950, and 1698 cm^{-1}, respectively. The phthalocyanines display typical UV-Vis spectra with two strong absorption regions, one of them in the UV region at about 300-350 nm (B-band) and the other one in the visible region at 600-700 nm (Q-band).[38,39] UV-Vis spectra of phthalocyanine-

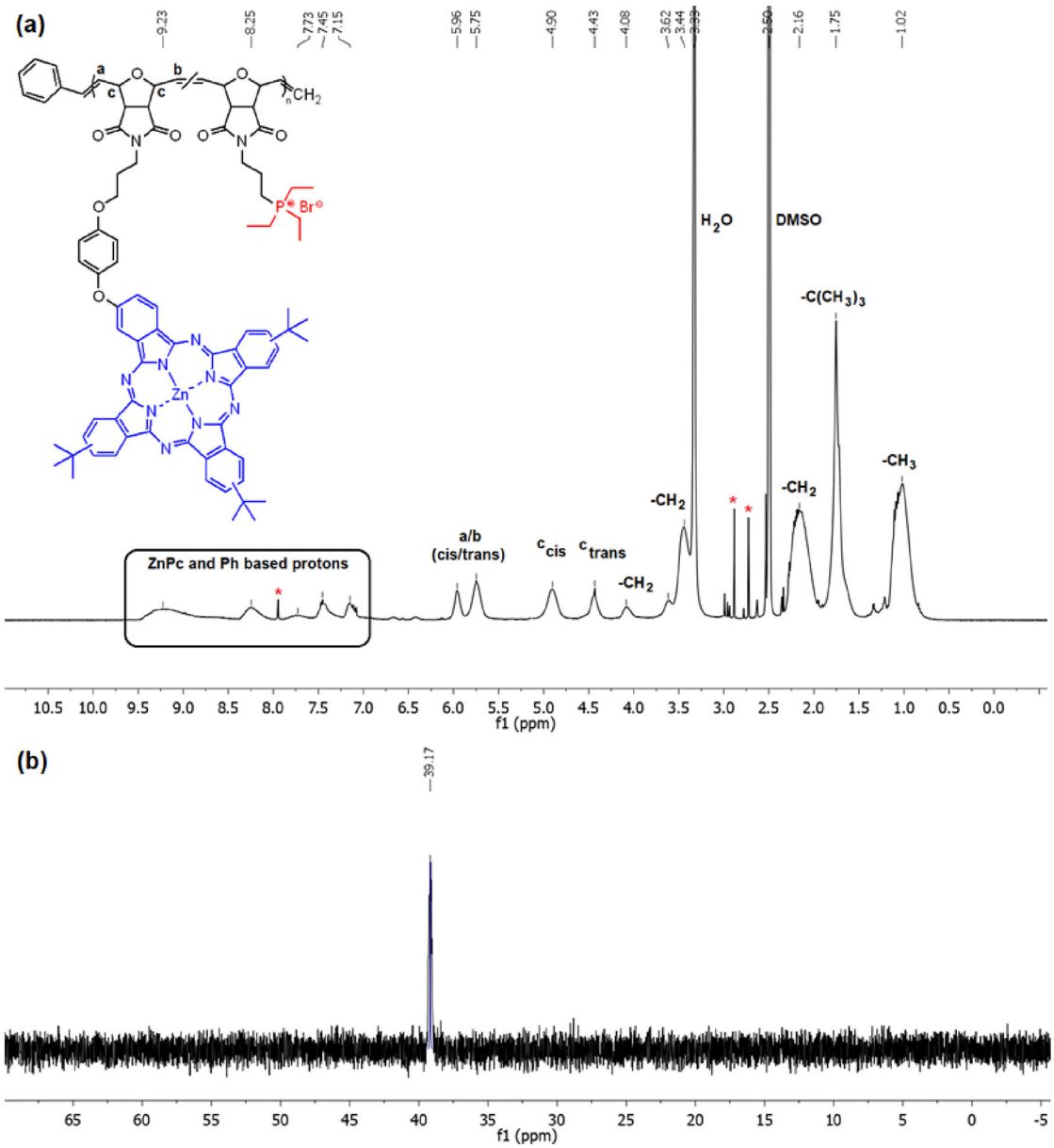

Figure 2. **(a)** ^{1}H-NMR spectrum of **P6** **(b)** ^{31}P-NMR spectrum of **P6**. * Indicates DMF peaks.

triethylphosphonium copolymers **P6** and **P7** were recorded in dimethyl sulfoxide (DMSO) at the same concentration. **P6** and **P7** have almost same absorption bands at ~350, 613, and 678 nm. UV-Vis spectra also showed that as the phthalocyanine molar ratio in the polymer increased, the intensity of the Q-band at 678 nm increased. This result is in harmony with the molecular composition of the polymers.[40] Molecular weight analysis was conducted by using SEC technique and MALDI-TOF MS. However, we could not get signal except SEC with DMF mobile phase, but the polymers' molecular weight deviate enormously from the theoretical values of M_n.

3.2. Physicochemical properties

3.2.1. Fluorescence quantum yields (Φ_F), emission and lifetimes

The absorption, fluorescence emission and excitation spectra of the copolymers are shown in Figure 3 to illustrate the

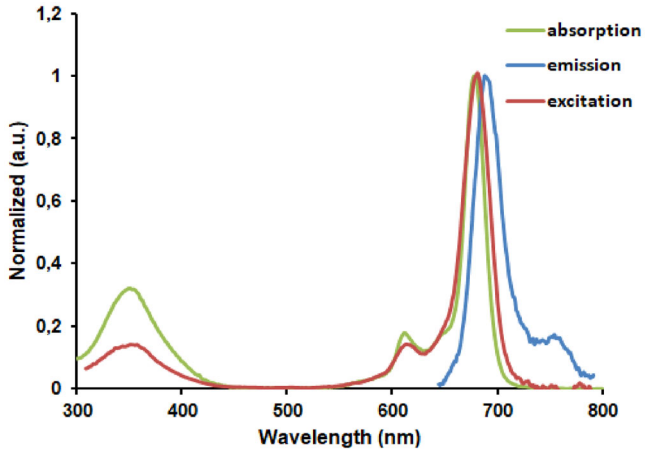

Figure 3. Absorption, excitation and emission spectra of **P6** (Excitation wavelength: 609 nm).

Table 1. Photophysicochemical parameters of **P6** and **P7** in DMSO and aqueous media (aq.).

Polymer	Solvent	Abs.	Exc.	Em.	Φ_F	Stokes shift Δ_{Stokes}, nm	Φ_Δ	τ_F (ns)	Φ_T	τ_T (μs)
P6	DMSO	678	681	690	0.045	9	0.22	2.65	0.25	88
P6	Aq.	633.679	–	–	<0.01	–	0.030	–	–	–
P7	DMSO	678	682	689	0.063	7	0.20	2.82	0.22	69
P7	Aq.	634.678	–	–	<0.01	–	0.035	–	–	–

measurements for compound **P6** as an example. Fluorescence behaviors of **P6** and **P7** were studied in DMSO and aqueous media and the related data were listed in Table 1.

The copolymers **P6** and **P7** were excited at 609 nm and 608 nm, respectively. The fluorescence emission wavelengths of the studied copolymers were determined at 681 nm for **P6** and 682 nm for **P7** in DMSO. When the fluorescence intensity of **P6** and **P7** against the wavelength is plotted, the emission spectrum is the mirror image of the absorption spectrum. The symmetric appearance of these spectra is a result of the same transitions being involved in both absorption and emission.[41] The excitation spectrum of copolymers (**P6**, **P7**) is slightly red-shifted compared to its absorption spectrum, which can be attributed slight aggregation in its ground state.[42] In addition, the observed Stokes shifts were 9 nm for **P6** and 7 nm for **P7**.

The fluorescence quantum yield (Φ_F) is the number of the absorbed light into emitted light. The comparative method was utilized to determine the fluorescence quantum yield of the studied polymers.[43] Unsubstituted ZnPc was utilized as a standard with the value: $\Phi_F = 0.2$.[40] The fluorescence quantum yields (Φ_F) for **P6** and **P7** were determined in DMSO and in water containing 5% DMSO for comparison purpose. The observed Φ_F values performed in DMSO were 0.045 for **P6** and 0.063 for **P7** (Table 1). All the studied copolymers showed lower fluorescence quantum yield than unsubstituted ZnPc standard in DMSO. This indicates the presence of the substituents causes the quenching of the fluorescence. The water-soluble positively charged **P6** and **P7** were also studied in aqueous media and it was seen that they were not fluorescent. It could be attributed to quenching effect of water which increases the aggregation causing the inactivation of the photoactivity of the molecules through dissipation of energy.[44] The values of Φ_F were evaluated by comparison with the reported polymers contain zinc phthalocyanines. Similar results were obtained with the poly(ethylene glycol) conjugated symmetrical and unsymmetrical zinc phthalocyanines.[45] In contrast, polyethylenimine (PEI) with zinc phthalocyanine side chains showed higher fluorescence quantum yield, in relation to whether it creates aggregation in the solution medium.[46]

Fluorescence lifetime values shows the duration time of the absorbed photons in the excited state before returning to the ground state after excitation. Fluorescence lifetime values (τ_F) of the **P6** and **P7** were measured in DMSO by TCSPC (time correlated single photon counting) method which is a counting process. The determined τ_F values are 2.65 ns for **P6** and 2.82 ns for **P7** (Table 1). The illustrated fluorescence mono-exponential decay curve as an example with their corresponding residual graph in DMSO for copolymer **P6** is shown in Figure 4.

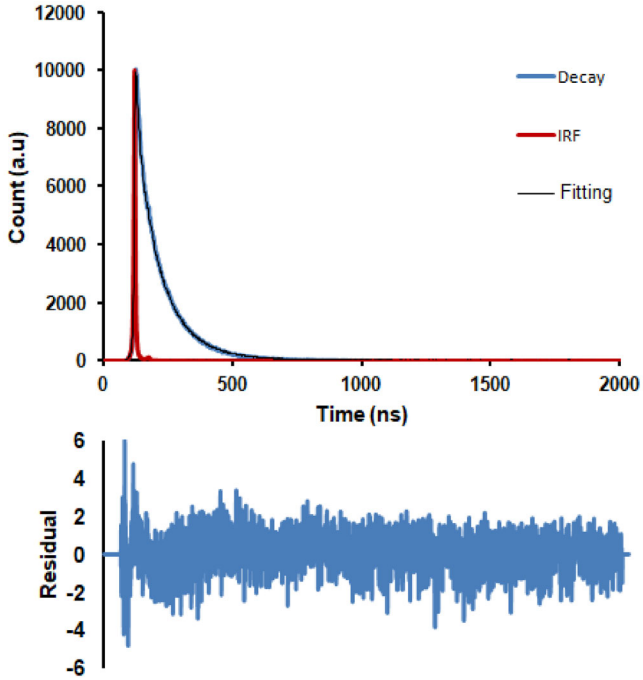

Figure 4. Fluorescence decay (blue), $\chi 2$ fitting (black) and IRF (red) curves for **P6** in DMSO (as an example).

3.2.2. Singlet oxygen quantum yields (Φ_Δ)

The efficiency of the photodynamic process is measured by the efficiency of the produced singlet oxygen ($^1O_2$) that is toxic species for cancer or microbial cells during the photochemical reactions.[47] The amount of generated singlet oxygen quantified as singlet oxygen quantum yield (Φ_Δ) under light irradiation. The observed singlet oxygen quantum yield indicate the effectiveness of the photosensitizers before cell studies for PDT applications.[48]

The determination of $^1O_2$ quantum yield was carried out with the comparative method using standard samples with known $^1O_2$ quantum yields such as unsubstituted ZnPc ($\Phi_\Delta = 0.67$ in DMSO)[49] and AlPcSmix (containing a mixture of differently sulfonated phthalocyanines) ($\Phi_\Delta = 0.42$ in aqueous media).[50] This chemical method requires the use of DPBF (in DMSO) and ADMA (in aqueous media) as singlet oxygen quenchers. The decay of the singlet oxygen quenchers was monitored with the UV-Vis spectroscopy in DMSO and in water (5% DMSO) solutions for comparative purpose under identical conditions with the experimental set-up described in the literature.[51] Figure 5 is shown as examples exhibiting the absorbance changes of DPBF (a) and ADMA (b) at various time intervals for compound **P6**. Studied poly(oxanorbornene)s containing pendant zinc(II) phthalocyanine did not show any changes on the Q bands in terms of the intensities or shapes. That indicate the **P6** and **P7** are stable under light illumination.[52]

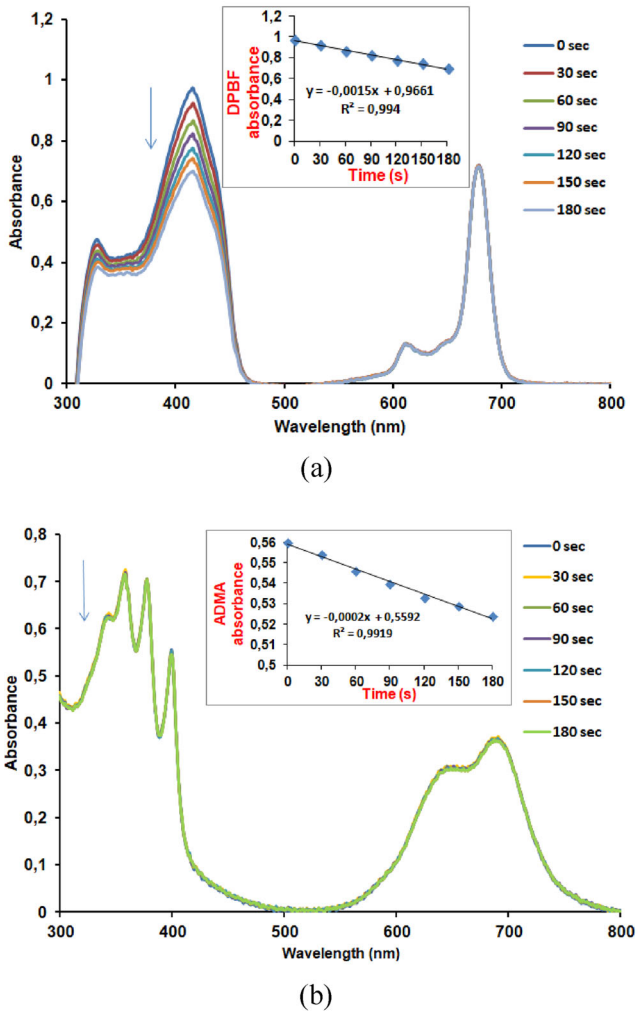

Figure 5. Representative absorption spectral changes during the determination of singlet oxygen quantum yield of **P6** (a) in DMSO using DPBF, (b) in aqueous solution using ADMA (Inset: plot of changes of the DPBF/ADMA absorbances versus time).

Table 1 shows the value of Φ_Δ performed in both DMSO and aq. media. The copolymer **P7** displayed a little bit to lower singlet oxygen generation in DMSO with a value: Φ_Δ = 0.20 compared to **P6**. As the triethylphosphonium molar ratio in the polymer increased, the singlet oxygen quantum yield (Φ_Δ) value slightly increased to 0.22 for **P6** in DMSO. It could be attributed to the presence of more cationic ions increasing the electron density.[53] The observed smallest value in water (containing 5% DMSO) is due to aggregation tendency of **P6** and **P7** in aqueous media and also oxygen has lower solubility in water compared to organic solvents (Table 1).[54]

3.2.3. Triplet quantum yield (Φ_T) and lifetimes (τ_T)

The triplet state quantum yield (Φ_T) is an crucial property of the photosensitizers for PDT applications. It shows the fraction of molecules that undergoes the intersystem crossing to the triplet excited state where the energy transfer carry out from the triplet excited photosensitizer to molecular oxygen to form $^1O_2$.

The triplet quantum yield (Φ_T) and triplet lifetimes values of the **P6** and **P7** were determined using comparative methods defined in the literature using a laser flash photolysis system by employing the unsubstituted ZnPc as a standard in DMSO (Φ_T = 0.65).[49] The measurements of the samples were done in DMSO in the absence of oxygen by purging with nitrogen. Triplet lifetimes were determined by exponential fitting of the kinetic curves using OriginPro 7.5 software. The obtained results for Φ_T and τ_T are shown in Table 1. The triplet decay curve of **P6** as an example is shown in Figure 6. **P6** obeyed second order kinetics, typical of MPcs at high concentration, due to triplet–triplet recombination.[55]

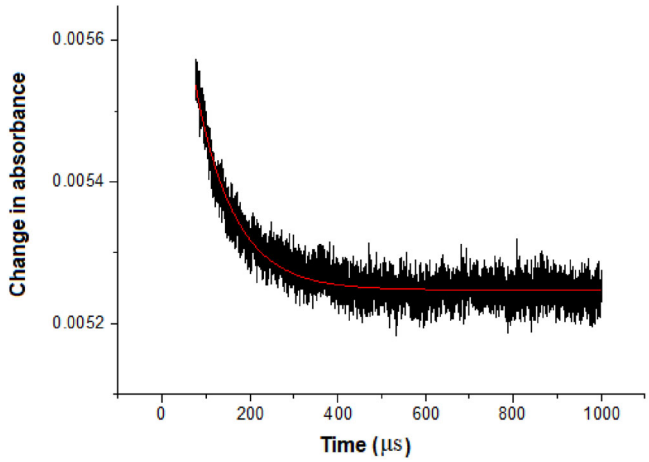

Figure 6. Triplet absorption decay (black) and fitting (red) curve for **P6** (solvent = DMSO).

The copolymers **P6** and **P7** displayed moderate triplet quantum yield (Φ_T) with the value of 0.25 and 0.22, respectively. Increasing the ratio of the triethylphosphonium unit in the polymer promotes intersystem crossing to the triplet state more efficiently resulting the more populated triplet excited photosensitizer in this state. The triplet quantum yield (Φ_T) values followed the same trend with singlet oxygen quantum yield values. A high triplet quantum yield leads to high singlet oxygen generation. High triplet quantum yield (Φ_T) values accompanied by high triplet lifetimes.[56] The triplet lifetimes were observed as 88 μs for **P6** and 69 μs for **P7** (Table 1).

3.2.4. Cell studies

Dark and light toxicity studies of **P1**-**P7** were performed *in vitro* on MCF-7 cancer cells by quantification of surviving cells using the WST-1 cell proliferation assay 24 h after the treatment with 0–60 μg/mL concentrations of **P1**-**P7**. The *in vitro* dark cytotoxicity studies and *in vitro* PDT evaluation of the photosensitizer was carried out at the same concentrations and experimental conditions. Figure 7 as bar graph shows the *in vitro* dark cytotoxicity and PDT activity for polymers (**P1**-**P7**). For the highest concentrations (> 60 μM) significant increase in viability was observed for all tested conditions. All samples exhibit relatively moderate dark toxicity with dead cell percentage between approx. 25-50% in the absence of irradiation over the 0–60 μg mL^{-1} concentration range (Figure 7a). The phototoxicity activity of complexes was found to increase with increase in concentration as evidenced by decrease in cell viability (Figure 7b).

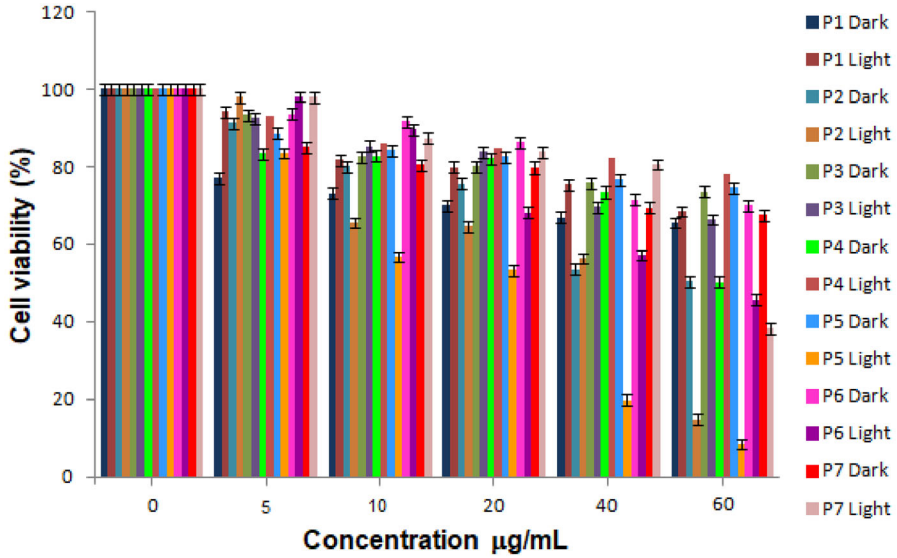

(a)

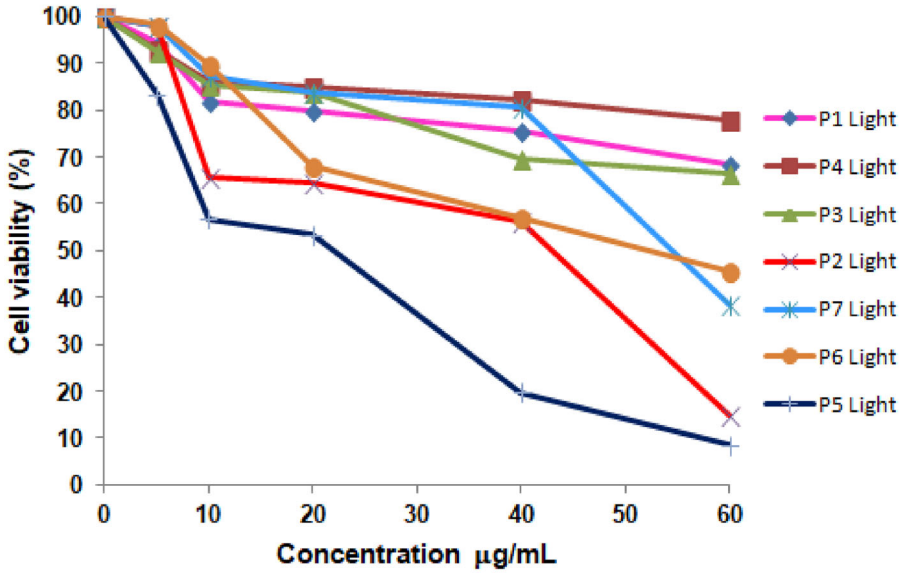

(b)

Figure 7. Cell viability determined following cytotoxicity (dark) and photocytotoxicity (light) experiments, (a) photocytotoxicity (light) experiments (b) of polymers (**P1**-**P7**) activity against MCF-7 cells as determined with the WST-1 assay.

P5 exhibit extremely high PDT activity at the highest tested concentration of 60 μg/mL with 8.43% cell viability while the percentage cell viability was observed as 68.46% for **P1**, 14.77% for **P2**, 66.47% for **P3**, 78.02% for **P4**, 45.68% for **P6** and 38.34% for **P7**. When comparing the results in terms of substituents, regardless of phenyl or ethyl groups, as the number of positively charged phosphonium functionalities increased as in **P2** and **P5**, enhanced PDT activity was observed.[57] Although all the studied polymers (**P1**-**P7**) showed similar singlet oxygen quantum yield,[33] previous studies reported that the PDT activity of the photosensitizers not only depend on the singlet oxygen production but also depend on the cell type, cellular uptake and localization.[58] These factors can be directly affect the response of the cell.

4. Conclusions

We presented the use of PDT as a therapeutic approach in the treatment of human breast adenocarcinoma cell line (MCF-7 cells) in addition to the photophysicochemical properties of the macromolecular photosensitizers based on poly(oxanorbornene) with zinc(II) phthalocyanine side chains. They all showed *in vitro* light toxicity with the range of 20-90% dead cells in all the tested concentrations. **P2** and **P5** containing more positively charged triphenyl/ethyl phosphonium group on the molecule showed enhanced PDT activity compared to others containing less positively charged group and neutral polymer **P1**. It might be attributed to the enhanced singlet oxygen quantum yield, especially for **P5**.

Funding

The authors would like to acknowledge the financial support from The Scientific and Technological Research Council of Turkey (TÜBİTAK) (Project Number: 219Z271).

References

[1] Wang, Z.; Gai, S.; Wang, C.; Yang, G.; Zhong, C.; Dai, Y.; He, F.; Yang, D.; Yang, P. Self-Assembled Zinc Phthalocyanine Nanoparticles as Excellent Photothermal/Photodynamic Synergistic Agent for Antitumor Treatment. *Chem. Eng. J.* **2019**, *361*, 117–128. DOI: 10.1016/j.cej.2018.12.007.

[2] Yang, D.; Yang, G.; Yang, P.; Lv, R.; Gai, S.; Li, C.; He, F.; Lin, J. Assembly of Au Plasmonic Photothermal Agent and Iron Oxide Nanoparticles on Ultrathin Black Phosphorus for Targeted Photothermal and Photodynamic Cancer Therapy. *Adv. Funct. Mater.* **2017**, *27*, 1700371. DOI: 10.1002/adfm.201700371.

[3] Cui, D.; Huang, J.; Zhen, X.; Li, J.; Jiang, Y.; Pu, K. A Semiconducting Polymer Nano-prodrug for Hypoxia-Activated Photodynamic Cancer Therapy. Angew. Chem. Int. Ed. Engl. **2019**, *58*, 5920–5924. DOI: 10.1002/anie.201814730.

[4] Dolmans, D. E.; Fukumura, D.; Jain, R. K. Photodynamic Therapy for Cancer. *Nat Rev Cancer* **2003**, *3*, 380–387. DOI: 10.1038/nrc1071.

[5] Lovell, J. F.; Liu, T. W.; Chen, J.; Zheng, G. Activatable Photosensitizers for Imaging and Therapy. Chem. Rev. **2010**, *110*, 2839–2857. DOI: 10.1021/cr900236h.

[6] Li, X.; Zheng, B.-D.; Peng, X.-H.; Li, S.-Z.; Ying, J.-W.; Zhao, Y.; Huang, J.-D.; Yoon, J. Phthalocyanines as Medicinal Photosensitizers: Developments in the Last Five Years. Coord. Chem. Rev. **2019**, *379*, 147–160. DOI: 10.1016/j.ccr.2017.08.003.

[7] Wang, C.; Qian, Y. A Water Soluble carbazolyl-BODIPY Photosensitizer with an Orthogonal D-A Structure for Photodynamic Therapy in Living Cells and Zebrafish. Biomater. Sci. **2020**, *8*, 830–836. DOI: 10.1039/c9bm01709g.

[8] Linden, G.; Vázquez, O. Bioorthogonal Turn-On BODIPY-Peptide Photosensitizers for Tailored Photodynamic Therapy. *Chemistry* **2020**, *26*, 10014–10023. DOI: 10.1002/chem.202001718.

[9] Zhang, H.; Bo, S.; Zeng, K.; Wang, J.; Li, Y.; Yang, Z.; Zhou, X.; Chen, S.; Jiang, Z.-X. Fluorinated Porphyrin-Based Theranostics for Dual Imaging and Chemo-Photodynamic Therapy. J. Mater. Chem. B. **2020**, *8*, 4469–4474. DOI: 10.1039/d0tb00083c.

[10] Mahajan, P. G.; Dige, N. C.; Vanjare, B. D.; Kim, C.-H.; Seo, S.-Y.; Lee, K. H. Design and Synthesis of New Porphyrin Analogues as Potent Photosensitizers for Photodynamic Therapy: Spectroscopic Approach. J. Fluoresc. **2020**, *30*, 397–410. DOI: 10.1007/s10895-020-02513-2.

[11] Ferreira, J. T.; Pina, J.; Ribeiro, C. A.; Fernandes, R.; Tomé, J. P.; Rodríguez-Morgade, M. S.; Torres, T. Highly Efficient Singlet Oxygen Generators Based on Ruthenium Phthalocyanines: Synthesis, Characterization and in Vitro Evaluation for Photodynamic Therapy. *Chemistry* **2020**, *26*, 1697–1697. DOI: 10.1002/chem.201905549.

[12] Revuelta-Maza, M. Á.; Mascaraque, M.; González-Jiménez, P.; González-Camuñas, A.; Nonell, S.; Juarranz, Á.; De La Torre, G.; Torres, T. Assessing Amphiphilic ABAB Zn (II) Phthalocyanines with Enhanced Photosensitization Abilities in in Vitro Photodynamic Therapy Studies against Cancer. *Molecules* **2020**, *25*, 213. DOI: 10.3390/molecules25010213.

[13] Motloung, B. M.; Babu, B.; Prinsloo, E.; Nyokong, T. The Photophysicochemical Properties and Photodynamic Therapy Activity of in and Zn Phthalocyanines When Incorporated into Individual or Mixed Pluronic® Micelles. *Polyhedron* **2020**, *188*, 114683. DOI: 10.1016/j.poly.2020.114683.

[14] Li, X.; Park, E. Y.; Kang, Y.; Kwon, N.; Yang, M.; Lee, S.; Kim, W. J.; Kim, C.; Yoon, J. Supramolecular Phthalocyanine Assemblies for Improved Photoacoustic Imaging and Photothermal Therapy. *Angew. Chem.* **2020**, *132*, 8708–8712. DOI: 10.1002/ange.201916147.

[15] Bispo, M.; Pereira, P. M.; Setaro, F.; Rodríguez-Morgade, M. S.; Fernandes, R.; Torres, T.; Tomé, J. P. A Galactose Dendritic Silicon (IV) Phthalocyanine as a Photosensitizing Agent in Cancer Photodynamic Therapy. Chempluschem. **2018**, *83*, 855–860. DOI: 10.1002/cplu.201800370.

[16] Ogawara, K.; Shiraishi, T.; Araki, T.; Watanabe, T.; Ono, T.; Higaki, K. Efficient anti-Tumor Effect of Photodynamic Treatment with Polymeric Nanoparticles Composed of Polyethylene Glycol and Polylactic Acid Block Copolymer Encapsulating Hydrophobic Porphyrin Derivative. Eur. J. Pharm. Sci. **2016**, *82*, 154–160. DOI: 10.1016/j.ejps.2015.11.016.

[17] Figueira, F.; Pereira, P.; Silva, S.; Cavaleiro, J.; Tome, J. Porphyrins and Phthalocyanines Decorated with Dendrimers: Synthesis and Biomedical Applications. *COS.* **2014**, *11*, 110–126. DOI: 10.2174/15701794113106660089.

[18] Tijerina, M.; Kopečková, P.; Kopeček, J. Mechanisms of Cytotoxicity in Human Ovarian Carcinoma Cells Exposed to Free Mce6 or HPMA Copolymer–Mce6 Conjugates. Photochem. Photobiol. **2003**, *77*, 645–652. DOI: 10.1562/0031-8655(2003)077<0645:MOCIHO > 2.0.CO;2.

[19] Yhee, J. Y.; Son, S.; Son, S.; Joo, M. K.; Kwon, I. C. The EPR Effect in Cancer Therapy. In *Cancer Targeted Drug Delivery: An Elusive Dream*; Bae, Y. H., Mrsny, R. J., Park, K., Eds.; Springer: New York, NY, 2013; pp 621–632.

[20] Maeda, H. Macromolecular Therapeutics in Cancer Treatment: The EPR Effect and beyond. *J. Control Release* **2012**, *164*, 138–144. DOI: 10.1016/j.jconrel.2012.04.038.

[21] Meng, Z.; Hou, W.; Zhou, H.; Zhou, L.; Chen, H.; Wu, C. Therapeutic Considerations and Conjugated Polymer-Based Photosensitizers for Photodynamic Therapy. *Macromol. Rapid Commun.* **2018**, *39*, 1700614. DOI: 10.1002/marc.201700614.

[22] Lu, Z.; Zhang, X.; Wu, Z.; Zhai, T.; Xue, Y.; Mei, L.; Li, C. BODIPY-Based Macromolecular Photosensitizer with Selective Recognition and Enhanced Anticancer Efficiency. *RSC Adv.* **2014**, *4*, 19495–19501. DOI: 10.1039/c4ra01412j.

[23] Shiah, J.; Sun, Y.; Peterson, C.; Straight, R.; Kopeček, J. Antitumor Activity of HPMA Copolymer Mesochlorin e 6 and Adriamycin in Combination Treatments. *Clin. Cancer Res.* **2000**, *6*, 1008–1015.

[24] Zhang, F. L.; Huang, Q.; Liu, J. Y.; Huang, M. D.; Xue, J. P. Molecular-Target-Based Anticancer Photosensitizer: Synthesis and In vitro Photodynamic Activity of Erlotinib-Zinc(II) Phthalocyanine Conjugates. *ChemMedChem.* **2015**, *10*, 312–320. DOI: 10.1002/cmdc.201402373.

[25] Kiew, L. V.; Cheah, H. Y.; Voon, S. H.; Gallon, E.; Movellan, J.; Ng, K. H.; Alpugan, S.; Lee, H. B.; Dumoulin, F.; Vicent, M. J.; Chung, L. Y. Near-Infrared Activatable Phthalocyanine-poly-L-Glutamic Acid Conjugate: increased Cellular Uptake and Light–Dark Toxicity Ratio toward an Effective Photodynamic Cancer Therapy. Nanomed. Nanotechnol. Biol. Med. **2017**, *13*, 1447–1458. DOI: 10.1016/j.nano.2017.02.002.

[26] Rosenkranz, A. A.; Jans, D. A.; Sobolev, A. S. Targeted Intracellular Delivery of Photosensitizers to Enhance Photodynamic Efficiency. *Immunol. Cell Biol.* **2000**, *78*, 452–464. DOI: 10.1046/j.1440-1711.2000.00925.x.

[27] Szewczyk, A.; Wojtczak, L. Mitochondria as a Pharmacological Target. Pharmacol. Rev. **2002**, *54*, 101–127. DOI: 10.1124/pr.54.1.101.

[28] Pathania, D.; Millard, M.; Neamati, N. Opportunities in Discovery and Delivery of Anticancer Drugs Targeting Mitochondria and Cancer Cell Metabolism. *Adv. Drug Deliv. Rev.* **2009**, *61*, 1250–1275. DOI: 10.1016/j.addr.2009.05.010.

[29] Liu, C.; Liu, B.; Zhao, J.; Di, Z.; Chen, D.; Gu, Z.; Li, L.; Zhao, Y. Nd3+ -Sensitized Upconversion Metal-Organic Frameworks for Mitochondria-Targeted Amplified Photodynamic Therapy .

Angew. Chem. Int. Ed. Engl. **2020**, *59*, 2634–2638. DOI: 10.1002/anie.201911508.

[30] Zhao, Z.; Chan, P.-S.; Li, H.; Wong, K.-L.; Wong, R. N. S.; Mak, N.-K.; Zhang, J.; Tam, H.-L.; Wong, W.-Y.; Kwong, D. W. J.; Wong, W.-K. Highly Selective Mitochondria-Targeting Amphiphilic Silicon(IV) Phthalocyanines with Axially Ligated Rhodamine B for Photodynamic Therapy. Inorg. Chem. **2012**, *51*, 812–821. DOI: 10.1021/ic201178e.

[31] Muli, D. K.; Rajaputra, P.; You, Y.; McGrath, D. V. Asymmetric ZnPc–Rhodamine B Conjugates for Mitochondrial Targeted Photodynamic Therapy. Bioorg. Med. Chem. Lett. **2014**, *24*, 4496–4500. DOI: 10.1016/j.bmcl.2014.07.082.

[32] Tarhouni, M.; Durand, D.; Önal, E.; Aggad, D.; İşci, Ü.; Ekineker, G.; Brégier, F.; Jamoussi, B.; Sol, V.; Gary-Bobo, M.; Dumoulin, F. Triphenylphosphonium-Substituted Phthalocyanine: Design, Synthetic Strategy, Photoproperties and Photodynamic Activity. *J. Porphyrins Phthalocyanines* **2018**, *22*, 552–561. DOI: 10.1142/S1088424618500554.

[33] Ahmetali, E.; Sen, P.; Süer, N. C.; Aksu, B.; Nyokong, T.; Eren, T.; Şener, M. K. Enhanced Light-Driven Antimicrobial Activity of Cationic Poly (Oxanorbornene) s by Phthalocyanine Incorporation into Polymer as Pendants. *Macromol. Chem. Phys.* **2020**, *221*, 2000386. DOI: 10.1002/macp.202000386.

[34] Süer, N. C.; Demir, C.; Ünübol, N. A.; Yalçın, Ö.; Kocagöz, T.; Eren, T. Antimicrobial Activities of Phosphonium Containing Polynorbornenes. *RSC Adv.* **2016**, *6*, 86151–86157. DOI: 10.1039/C6RA15545F.

[35] Sen, P.; Managa, M.; Nyokong, T. New Type of Metal-Free and Zinc (II), in (III), Ga (III) Phthalocyanines Carrying Biologically Active Substituents: synthesis and Photophysicochemical Properties and Photodynamic Therapy Activity. Inorg. Chim. Acta **2019**, *491*, 1–8. DOI: 10.1016/j.ica.2019.03.010.

[36] Mohammed, I.; Oluwole, D. O.; Nemakal, M.; Sannegowda, L. K.; Nyokong, T. Investigation of Novel Substituted Zinc and Aluminium Phthalocyanines for Photodynamic Therapy of Epithelial Breast Cancer. *Dyes Pigm.* **2019**, *170*, 107592. DOI: 10.1016/j.dyepig.2019.107592.

[37] Williams, D. N.; Saar, J. S.; Bleicher, V.; Rau, S.; Lienkamp, K.; Rosenzweig, Z. Poly(oxanorbornene)-Coated CdTe Quantum Dots as Antibacterial Agents . *ACS Appl. Bio. Mater.* **2020**, *3*, 1097–1104. DOI: 10.1021/acsabm.9b01045.

[38] Korkut, S. E.; Akyüz, D.; Özdoğan, K.; Yerli, Y.; Koca, A.; Şener, M. K. TEMPO-Functionalized Zinc Phthalocyanine: synthesis, Magnetic Properties, and Its Utility for Electrochemical Sensing of Ascorbic Acid. *Dalton Trans.* **2016**, *45*, 3086–3092. DOI: 10.1039/c5dt04513d.

[39] Dinçer, H. A.; Şener, M. K.; Koca, A.; Gül, A.; Koçak, M. B. Synthesis, Electrochemistry and in Situ Spectroelectrochemistry of Soluble Lead Phthalocyanines. Electrochim. Acta **2008**, *53*, 3459–3467. DOI: 10.1016/j.electacta.2007.11.060.

[40] de la Escosura, A.; Martínez-Díaz, M. V.; Torres, T.; Grubbs, R. H.; Guldi, D. M.; Neugebauer, H.; Winder, C.; Drees, M.; Sariciftci, N. S. New Donor-Acceptor Materials Based on Random Polynorbornenes Bearing Pendant Phthalocyanine and Fullerene Units. *Chem. Asian J.* **2006**, *1*, 148–154. DOI: 10.1002/asia.200600090.

[41] Lakowicz, J. R. *Principles of Fluorescence Spectroscopy*; Springer science & business media: New York, 2013.

[42] Ogunsipe, A.; Chen, J.-Y.; Nyokong, T. Photophysical and Photochemical Studies of Zinc (II) Phthalocyanine Derivatives—Effects of Substituents and Solvents. *New J. Chem.* **2004**, *28*, 822–827. DOI: 10.1039/B315319C.

[43] Williams, A. T. R.; Winfield, S. A.; Miller, J. N. Relative Fluorescence Quantum Yields Using a Computer-Controlled Luminescence Spectrometer. *Analyst* **1983**, *108*, 1067–1071. DOI: 10.1039/an9830801067.

[44] Nyokong, T. Effects of Substituents on the Photochemical and Photophysical Properties of Main Group Metal Phthalocyanines. Coord. Chem. Rev. **2007**, *251*, 1707–1722. DOI: 10.1016/j.ccr.2006.11.011.

[45] Dinçer, H.; Mert, H.; Çalış, E.; Atmaca, G. Y.; Erdoğmuş, A. Synthesis and Photophysicochemical Studies of Poly(Ethylene Glycol) Conjugated Symmetrical and Asymmetrical Zinc Phthalocyanines. J. Mol. Struct. **2015**, *1102*, 190–196. DOI: 10.1016/j.molstruc.2015.08.067.

[46] Baigorria, E.; Milanesio, E. M.; Durantini, E. N. Synthesis, Spectroscopic Properties and Photodynamic Activity of Zn(II) Phthalocyanine Polymer Conjugates as Antimicrobial Agents. Eur. Polym. J. **2020**, *134*, 109816. DOI: 10.1016/j.eurpolymj.2020.109816.

[47] Nyokong, T. Desired Properties of New Phthalocyanines for Photodynamic Therapy. *Pure & Appl. Chem.* **2011**, *83*, 1763–1779. DOI: 10.1351/PAC-CON-10-11-22.

[48] Maria, C.; DeRosa, R. J. C. Photosensitized Singlet Oxygen and Its Applications. *Coordination Chem. Rev.* **2002**, *233-234*, 351–371. DOI: 10.1016/S0010-8545(02)00034-6.

[49] Nyokong, T.; Antunes, E. Photochemical and Photophysical Properties of Metallophthalocyanines. In *Handbook of Porphyrin Science (Volume 7) with Applications to Chemistry, Physics, Materials Science, Engineering, Biology and Medicine*; World Scientific: Singapore, 2010; pp 247–357.

[50] Kuznetsova, N.; Gretsova, N.; Yuzhakova, O.; Negrimovskii, V.; Kaliya, O.; Luk'Yanets, E. New Reagents for Determination of the Quantum Efficiency of Singlet Oxygen Generation in Aqueous Media. *Russian J. General Chem.* **2001**, *71*, 36–41. DOI: 10.1023/A:1012369120376.

[51] Spiller, W.; Kliesch, H.; Wöhrle, D.; Hackbarth, S.; Röder, B.; Schnurpfeil, G. Singlet Oxygen Quantum Yields of Different Photosensitizers in Polar Solvents and Micellar Solutions. *J. Porphyrins Phthalocyanines* **1998**, *2*, 145–158.

[52] Çakır, D.; Çakır, V.; Bıyıklıoğlu, Z.; Durmuş, M.; Kantekin, H. New Water Soluble Cationic Zinc Phthalocyanines as Potential for Photodynamic Therapy of Cancer. J. Organomet. Chem. **2013**, *745-746*, 423–431. DOI: 10.1016/j.jorganchem.2013.08.025.

[53] Chen, L.; Zhao, Y.; Sun, X.; Jiang, J.; Wu, F.; Wang, K. Synthesis, Singlet Oxygen Generation and DNA Photocleavage of *β*, *β*′-Conjugated Polycationic Porphyrins. *J. Porphyrins Phthalocyanines* **2019**, *23*, 655–663. DOI: 10.1142/S1088424619500378.

[54] Ramesh, H.; Mayr, T.; Hobisch, M.; Borisov, S.; Klimant, I.; Krühne, U.; Woodley, J. M. Measurement of Oxygen Transfer from Air into Organic Solvents. J. Chem. Technol. Biotechnol. **2016**, *91*, 832–836. DOI: 10.1002/jctb.4862.

[55] Debacker, M.; Deleplanque, O.; Van Vlierberge, B.; Sauvage, F. A Laser Photolysis Study of Triplet Lifetimes and of Triplet–Triplet Annihilation Reactions of Phthalocyanins in DMSO Solutions (Etude des Durées de Vie du Triplet et des Réactions d'Annihilation Triplet–Triplet de Phthalocyanines dans le DMSO par Photolyse Laser). *Laser Chem.* **1988**, *8*, 1–11. DOI: 10.1155/LC.8.1.

[56] Darwent, J. R.; McCubbin, I.; Phillips, D. Excited Singlet and Triplet State Electron-Transfer Reactions of Aluminium (III) Sulphonated Phthalocyanine. *J. Chem. Soc, Faraday Trans. 2.* **1982**, *78*, 347–357. DOI: 10.1039/f29827800347.

[57] Matshitse, R.; Nwaji, N.; Mananga, M.; Prinsloo, E.; Nyokong, T. Effect of Number of Positive Charges on the Photophysical and Photodynamic Therapy Activities of Quarternary Benzothiazole Substituted Zinc Phthalocyanine. J. Photochem. Photobiol, A. **2018**, *367*, 253–260. DOI: 10.1016/j.jphotochem.2018.08.033.

[58] Menard, J. A.; Christianson, H. C.; Kucharzewska, P.; Bourseau-Guilmain, E.; Svensson, K. J.; Lindqvist, E.; Indira Chandran, V.; Kjellén, L.; Welinder, C.; Bengzon, J.; et al. Metastasis Stimulation by Hypoxia and Acidosis-Induced Extracellular Lipid Uptake is Mediated by Proteoglycan-Dependent Endocytosis. *Cancer Res.* **2016**, *76*, 4828–4840. DOI: 10.1158/0008-5472.CAN-15-2831.